Journal of Cultural Heritage 75 (2025) 226–236

Contents lists available at ScienceDirect

Journal of Cultural Heritage

journal homepage: www.elsevier.com/locate/culher

Original article

Non-destructive, portable approach as pre-screening tool for archaeological burnt bones

Lucrezia Gatti[a], Zohreh Chahardoli[a], Giorgia Sciutto[a], Francesca Seghi[b], Antonino Vazzana[b], Stefano Benazzi[b], Lea Legan[c], Fabio Cavalli[d], Rocco Mazzeo[a], Silvia Prati[a,*]

[a] University of Bologna, Department of Chemistry "G. Ciamician", Ravenna Campus, Via Guaccimanni, 42, Ravenna 48121, Italy
[b] University of Bologna, Department of Cultural Heritage, Ravenna Campus, Via degli Ariani, 1, Ravenna 48121, Italy
[c] Institute for the Protection of Cultural Heritage of Slovenia, Conservation Centre, Poljanska cesta 40, Ljubljana 1000, Slovenia
[d] Research Unit of Paleoradiology and Allied Sciences, Laboratorio di Telematica Sanitaria-Struttura Complessa Informatica e Telecomunicazioni, Azienda Sanitaria Universitaria Giuliana Isontina, Trieste 34149, Italy

ARTICLE INFO

Article history:
Received 11 March 2025
Accepted 18 July 2025

Keywords:
Nir spectroscopy
Portable mid-FTIR
Principal component analysis
Burnt bones, Non-invasive analyses
Archaeological bones

ABSTRACT

Ancient bones are archives of information to reconstruct past life. However, detecting the organic content and the crystallinity changes of bone apatite post-mortem alteration becomes more challenging when burial conditions are coupled with thermal degradation. The present study proposed a non-invasive pre-screening method to distinguish burnt bones based on diagnostic spectral features, using a reflectance portable FT-IR spectrometer (650–5500 cm^{-1}) and a portable miniaturized near-infrared (MicroNIR) spectrometer (900–1700 nm). Burnt bones from the Roman age (Modena, Italy) were analyzed and the pre-screening approach was combined with a multivariate data analysis. Principal Component Analysis (PCA) was used to enhance spectral changes leading to a differentiation among the specimens, according to their chemical changes. The proposed methodology highlighted the potential of the two non-destructive and portable instruments, and of chemometric analysis to select the most suitable samples for forensic and archaeological studies, overcoming drawbacks related to the traditionally applied visual examination of bones colour.

1. Introduction

Bone is a composite material constituted by the intimate association of an organic component, a mineral phase and water [1–5] arranged in a complex structure described in terms of hierarchical levels of organization. The mineral fraction consists of bioapatite, (carbonate-substituted apatite, $Ca_{10}(PO_4, CO_3)_6(OH)_2$) [1,3–7], while the organic matrix is mainly collagen type I [5,6] accounting 30 % of total bone weight [2]. Bones could be an essential reservoir for the reconstruction of past human habits and history. However, bones are dynamic tissues that undergo constant remodeling both during life and post-mortem, due to burial effects [2,8,9]. Consequently, investigating bones becomes challenging for anthropologists when burial conditions are coupled with thermal degradation [2,10–14].

Burnt bones are observed in the archaeological record, resulting from heating practices, accidental exposure to fire, use of bone as fuel, or from mortuary practices, i.e. cremation, a common rite in many cultures and civilizations throughout history [15,16]. In its original state, bone exhibits a disordered crystal structure with small crystals [17]. The exposure of bones to high temperatures leads to different burning states [1,2,12–14,17,18] as an effect of:

- Dehydration, (100–600°C);
- Degradation and loss of organic matter (300–800°C);
- Increase in crystallinity of bioapatite and formation of stable and large crystals (inversion and fusion) (500–1100°C).

Moreover, when the water and organic components are lost, and thermal alteration is prolonged (over 800°C), fusion of crystals occurs and several degradation products appear, such as tricalcium (α- and ß-) and tetracalcium phosphates [2,5,12,14,18,19]. Consequently, the result of prolonged and intense thermal degradation is the formation of bioapatite (HA) [20].

Even if dating of cremated remains has become common [15,16,21–23], burnt remains are often excluded from advanced analyses for dating or molecular analyses, due to their structural alterations. However, in many archaeological sites, burnt bones are the only source of information. For this reason, a deeper under-

* Corresponding author.
E-mail address: s.prati@unibo.it (S. Prati).

https://doi.org/10.1016/j.culher.2025.07.021

Table 1
Reference samples burnt at known temperature and time.

Sample ID	Temperature (°C)	Exposure time (min.)
S1	/	/
S2	300	30
S3	300	60
S4	300	90
S5	300	120
S6	600	30
S7	600	60
S8	600	90
S9	600	120
S10	900	30
S11	900	60
S12	900	90
S13	900	120
S14	1200	30
S15	1200	60
S16	1200	90
S17	1200	120

standing of chemical changes of both organic and inorganic fractions in each burning phase is essential. Usually, preliminary investigations of burnt bones are based on the visual examination of the color change according to reference color charts as an indicator of the heat-induced transformations [2,12]. Indeed, when the temperature increases, bones acquire a black appearance due to carbonization. With further heating, the bones take on grey hues, until they get white due to calcination processes [1,2,14]. Besides the color changes, morphological modification can also be observed such as increase in the porosity and the brittleness [24].

Colorimetric investigations based on CIE L*a*b* (CIELAB) uniform color space was also used for the recording of bone surface color data [25–28]. However, since the color of bone fragments is produced by a combined effect of i) temperature, ii) time of exposure, iii) occurrence of oxidative conditions, and iiii) context of incineration [12,14,18], the color examination method may be ineffective in predicting the burning state of bones [17,29]. On the other hand, the identification of the burning state is crucial to evaluate which remains may be worthy to be selected for further investigation such as isotopic, dating, proteomic, and DNA analyses which are expensive and time consuming [5,6,30–32].

In recent years, Fourier transform infrared (FTIR) spectroscopy [1,2,5,17,33–36], both in the ATR [6,7,37], and reflection mode, in the mid-IR range has been employed to comprehensively monitor heat-induced chemical alterations in bone samples (Table 1). Infrared spectra provide information on both the organic and the inorganic components, such as the presence of phosphate from bioapatite (HA), of carbonate from the substitution in bioapatite of the hydroxyl and phosphate groups, and of amide bands from the proteinaceous component [6,17,33].

FTIR studies demonstrated that, even after thermal treatments, spectral signals from the organic component remain detectable up to 600 °C. In particular, below 300 °C, both amide I and II bands, along with signals attributed to the asymmetric vibration of CH_2 and symmetric vibration of CH_3, are observable. Between 300 and 600 °C, only the amide I can be detected. Beyond 600 °C, the organic fraction undergoes complete deterioration, and specific degradation products, notably low-intensity bands associated with cyanate (NCO^-) and cyanamide (NCN^{2-}), indicate an escalating heating process from 600 °C to 1000 °C, as a consequence of charring [2,38,39].

The mineral fraction of bones primarily composed of phosphates, shows a temperature-dependent stretching band at 1015 cm^{-1}. This band begins to shift to higher wavenumbers after 300 °C, moreover at 600 °C starts to bifurcate into two peaks likely due to increased crystallization. Thermal degradation products, such as α –and β -tricalcium phosphate result from the bone dehydroxylation process, which occurs at temperatures above 900 °C [2].

FTIR-ATR allows to obtain clear spectra with the consequent possibility to evaluate the Infrared Splitting factor (carbonyl-to-phosphate ratio) and carbonyl-to-carbonate ratio to assess the temperature [1,40,41], while the use of portable FTIR in reflection mode posed challenges, as surface modifications and sediment accumulation could obscure the signal, making it difficult to distinguish the bone signals. Reflectance spectra are more complex due to distortions arising from the combined effects of specular reflection (Rs) and volume reflection (Rv) contributing to the total reflected signal [42,43].

In recent studies, near infrared spectroscopy has been applied to human forensic burnt samples to differentiate between calcined and carbonized bones [14]. However, as far as the authors are aware, NIR spectroscopy has not been systematically employed in archaeological research to comprehensively investigate burnt bones, exploring its potential as a rapid and deeply penetrating analytical method. Interestingly, recent applications of NIR spectroscopy on animal and human bones have focused on assessing collagen presence and content, leveraging its ability to probe several millimeters beneath the surface [4,44–49].

Despite the widespread use of infrared spectroscopy in cultural heritage studies, archaeologists still rely on color-based assessments to determine burning phases.

The aim of this research was to propose a more objective prescreening method to evaluate burnt bones conservation state by means of a non-invasive, fast, and portable approach. To reach this goal two complementary techniques were used combined with a chemometric approach. In detail a handled miniaturized NIR spectrometer (MicroNIR), which works in the 900–1700 nm range and a non-contact reflectance portable FTIR spectrometer, which works in the 650–5500 cm^{-1} range, were used for a non-invasive, fast analysis.

First the two techniques were tested on the same standard samples used in Legan et al. [2], prepared on a modern bovine femur exposed to different controlled temperatures. Since the detailed identification of the burning conditions of the specimens is beyond the scope of the research, we limited the identification of the spectral features to these standards which were previously studied [2]. Thus, this preliminary characterization was aimed at identifying markers characteristic of different conservation states, particularly for the MicroNIR spectrometer, which currently has limited reference data available.

The spectral investigation was applied on a large collection of archeological samples from the Roman period (I century B.C.–II century A.C.). A multivariate exploratory analysis based on PCA (principal component analysis), was applied to separate the specimens which were distinguished based on their state of conservation through a joint evaluation of the loadings and of the comparison with the spectral features identified in the standards [3,4,14,49,50].

The specimens were also assessed with the traditional visual examination and the comparison of the results with the spectroscopic pre-screening allowed to confirm the importance of developing more objective diagnostic methods to avoid the dismissal of burned bones samples which may visually appear less preserved than their actual state.

2. Materials and methods

2.1. Standard samples

Seventeen samples were used as standards for Portable FTIR and MicroNIR analyses, to identify the main features for each in

the mid (650–4000 cm^{-1}) and NIR region (980–1700 nm). These samples were the same previously used in the study of Legan et al. [2] for the determination of the main markers in mid-IR. The bones come from an adult bovine femur diaphysis which was cut into 17 rectangular pieces (4.5 × 4 cm), out of these samples 16 were burnt in a temperature-controlled vented muffle furnace (Table 1). Each sample was stored in a dry environment within small perforated low-density polyethene (LDPE) bags until analysis (Fig. S1).

2.2. Archeological samples and visual examination

Fifteen burnt bone samples were collected from the Roman necropolis of Via Emilia Est–Via Cesena of *Mutina* (known today as Modena, Italy) (Fig. S2). Excess soil was drilled from the remains, and then the bones were gently brushed, followed by a light water wash. Subsequently, the bones were left to air-dry. Visual observation was performed at the BONES Lab (Laboratory of Osteoarchaeology and Paleoanthropology, Department of Cultural Heritage, University of Bologna), attributing the burning state through the comparison with the color chart reported in Walker et al. [12]. The comparison with this color chart is routinely used as a method for phase assignment.

2.3. Portable FTIR spectroscopy

Agilent Cary 630 FTIR (Agilent Technologies, Santa Clara, CA) portable mid-infrared spectrometer was used to collect spectra allowing analyses in the range from 4000 to 650 cm^{-1} with a spectral resolution of 4 cm^{-1} and 256 scans. The number of points for each sample ranged from 4 to 13, according to the samples size. Indeed, some real samples were smaller and/or had rougher surface, while others were larger and/or had smoother surface. The number of points was chosen to ensure adequate coverage of sample heterogeneity. Diffuse reflectance measurements were conducted directly on the external surface of the samples, and for background collection, a gold mirror was employed. The acquisitions were carried out using the Agilent MicroLab PC software (JDSU Corporation, Milpitas, CA).

2.4. MicroNIR spectroscopy

Near infrared analyses were performed using the portable Viavi MicroNIR 1700ES spectrometer (Viavi Solutions, JDSU Corporation, Milpitas, California), a spectrometer performing in the spectral region of 900–1700 nm (6000–11,000 cm^{-1}), with a spectral resolution of 6 nm. The instrument is based on a linear-variable filter (LVF) acting as the dispersing element. The LVF is linked directly to a 128-pixel linear Indium Gallium Arsenide (InGaAs) uncooled detector, resulting in a compact device. The radiation source consists of two tungsten light bulbs. The spot of analysis is approximately 3 mm in diameter. The spectral data were acquired with an integration time of 3 ms and 1000 scans, using the MicroNIR Pro version 2.5.1 software by Viavi. Prior to any analysis, background was collected both on air and using a NIR-reflectance standard with 99 % diffuse reflectance. Samples were subsequently placed directly in contact with the instrument.

2.5. Data analysis

The multivariate data analysis for all spectroscopic techniques was performed using Matlab routines (The Mathworks Inc., Natick, USA). Spectra corrections (pre-processing) were performed in order to remove unwanted effects. Portable FTIR data were denoised using Discrete Wavelet Transform (DWT). To correct the baseline shifts, a linear detrending transform was applied. No Kramers-Kronig (KK) transformation was applied since the spectra presents the coexistence of specular and diffuse components [42 ,43]. A Savitzky-Golay second derivative was applied to all MicroNIR spectra after data acquisition (third polynomial order, 11 data point gap) to correct baseline shift and drift and to enhance the signals. In the Results and Discussion section only averaged spectra will be reported in figures and tables for brevity and clarity.

The pre-processed data were then subjected to Principal Component Analysis (PCA), an unsupervised method that enables data exploration and identification of trends [4,44,51].

3. Results and discussion

3.1. Analyses of standard samples

Standard samples burnt at known temperatures and durations previously analyzed by Legan et al. [2] were submitted to portable FTIR in reflection mode and micro NIR analyses and the results were integrated and used to identify spectral features related to the conservation state of samples, according to their spectral features (Fig. S3-S20, Tables 2, 3 and S1).

The results are briefly discussed here in accordance with the objectives of the present research, which focuses on the development of a protocol based exclusively on the use of non-destructive and portable techniques suitable for *in situ* analyses. Therefore, information derived from micro-destructive techniques such as ATR and FTIR in transmission obtained by Legan and presented in the previous work [2], has been excluded from the evaluation.

Table 2 reports the main spectral features, combining samples that, despite being exposed to different burning conditions, appeared indistinguishable based on their spectral profiles.

A detailed comment on the spectral features is demanded in the supporting information with all the spectra (Fig. S3-S11).

The same standard samples analyzed with the portable FTIR were also analyzed with MicroNIR spectroscopy to identify specific features as discussed in the supporting info and reported in Table 3.

Standards providing the same spectral profiles were considered to have been exposed to conditions that, even if different in term of temperature and exposure, lead them to a similar state of conservation, defined as burning state (BS). Based on the similarities we grouped the standard samples in seven groups from the untreated sample (BS0) to the samples exposed to stronger conditions in term of temperatures and exposure times (BS6) (Table 4).

It is out of the purposes of this paper identifying the exact combustion conditions, but just to identify spectral features which may be useful to distinguish real samples based on their conservation state.

Comparing the results, it can be noted that FTIR is more useful for the characterization of high burning stages (BS≥5), thanks to the occurrence of characteristic features. On the contrary, MicroNIR can distinguish better from different stages below 900 °C, thanks to its deeper penetration depth in the sample.

This information is particularly valuable for samples treated at lower temperatures, where the presence of organic materials is observed.

Near-IR radiation penetrates more deeply than mid-IR radiation, making the information obtained more representative of the internal state of bones and thus more reliable for pre-screening sampling methods [52,53].

On the other side, as the temperature and exposure time increase, the surface of the specimen begins to darken, decreasing the spectroscopic signal obtained with both techniques. Despite the reduction in signal in NIR spectra, it is still possible to distinguish characteristic features for different specimens up to S9 BS4. At this point, the signal becomes so low that FTIR is more effective

Table 2
Groups identified based on portable FTIR analyses on standard burnt bones and bands assignment.

S1-S2 0–300° (30′)	S3-S5 300° (60–120′)	S6-S9 600° (30–120′)	-S10 900° (30′)	S11-S17 900° (60–120′)-1200 (30–120′)	Attribution
	3180	3180			ν(OH)
–	–	–	–	3650	ν(Ca-OH)
–	–	3572	3572	3571	ν(OH)
–	–	–	–	3544	ν(F-OH)
–	–	–	–	3496	ν(Cl-OH)
2916	2916	2916	2914	–	ν_{aym} (CH_2)
2849	2849	2849	2847	–	ν_{aym} (CH_3)
–	2204	2202	2204	2204	ν_3 (NCO^-)
–	–	2146, 2076, 2046	2145, 2077, 2048	2141, 2077–2079, 2046	$(PO_4)^{3-}$ 2 ν_3 overtones and ν_3 combinations
–	2016	2018	2022	2020–2014	ν_3 (NCN^{2-})
–	–	1984	1986, 1930	1986,1930	$(PO_4)^{3-}$ 2 ν_1
1690	1688	1679–1686	1682	–	ν ($C=O$) (amide I) / δ (OH) / ν ($C=C$) aromatic
1595–1560	1599–1596	–	–	–	ν (CN), δ (CNH) (amide II) / ν ($C=C$) aromatic
1435–1401	1448–1401	1448–1401	1448–1401	–	$(CO_3)^{2-}$ $\nu_{3\ asym}$
–	–	–	–	1095–1110	$(PO_4)^{3-}$ $\nu_{3\ asym}$
1030	1030	1034	1034	1036–1047	$(PO_4)^{3-}$ $\nu_{3\ asym}$

All the spectra were acquired in reflection mode and the reported values are in cm^{-1}. Standard samples that show the same characteristic peaks are reported in the same column, thus in the same burning stage.

Table 3
Groups identified based on the MicroNIR spectra acquired on standard burnt bones and bands assignment.

S1-S2	S3	S4-S5	S6-S7	S8-S9	S11-S17	Attribution
1583	1583	–		–	–	NH 1st overtone
1508	1508	1502		–	–	NH 2nd overtone
–	–	–	1484	–	1490	Mg-OH 1st overtone
				1434	1434	CO_3^{2-} substitution of OH
1422	1428	1428	1428		–	OH 1st overtone
–	–		–	1391	1378	OH combination ν_{sym}+ ν_{asym}
1347	1347	–	–		–	CH Combination (CH_3 – CH_2 – CH)
1273	–	–	–	–	–	CH 2nd overtone
1180	1180	–	–	–	-	CH 2nd overtone
1025	–	–	–	–	–	NH 2nd overtone
	1001	1007	1007	1013	–	combination of δ H-O-H + ν O-H
982	951	951	945	951	976	C-H 3rd overtone and/or O-H 2nd overtone

All the reported values are in nm. Standard samples that show the same characteristic peaks are reported in the same column, thus in the same burning stage.

Table 4
Grouping made on standard samples based on mid-IR and NIR: BS = burning state.

Sample ID	Temperature (°C)	Exposure time (min)	Portable FTIR	NIR
S1	/	/	BS0	BS0
S2	300	30		
S3	300	60	BS1-BS2	BS1
S4	300	90		BS2
S5	300	120		
S6	600	30	BS3-BS4	BS3
S7	600	60		
S8	600	90		BS4
S9	600	120		
S10	900	30	BS5	No signal
S11	900	60	BS6	BS6
S12	900	90		
S13	900	120		
S14	1200	30		
S15	1200	60		
S16	1200	90		
S17	1200	120		

Table 5
Grouping of the archeological burnt bone samples based on visual examination, portable FTIR (in reflection mode) assessment, and micro NIR.

Sample ID	Burning state (visual subdivision based on [12])	Burning state (portable FTIR)	Burning state (Micro-NIR)
M1	400–600 °C	BS0–2	BS1
M2	400–1000 °C	BS0–2	BS1
M3	300–500 °C	BS0–2	BS0–1
M4	400–600 °C	BS0–2	B0–1
M5	600–700 °C	BS0–2	BS1
M6	600–700 °C	BS5–6	NOISY
M7a	600–900 °C	BS0–2	BS2
M7b	600–900 °C	BS6	BS6
M8	300–500 °C	BS0–2	BS0–1
M9	400–500 °C	BS0–2	BS1
M10	300 °C	BS1–2	BS2
M11	400–800 °C	BS0–2	BS1
M12	700–900 °C	BS5–6	NOISY
M13	400–600 °C	BS0–2	BS1
M14	400–700 °C	BS5–6	NOISY
M15	400–700 °C	BS0–2	BS1

in distinguishing the burning state, at least at a superficial level. With further increases in temperature and/or exposure time, calcination occurs, and the surface acquires a white coloration. In this state, both FTIR and NIR spectra provide similar information, despite their depth of penetration, thereby highlighting a homogeneity in depth of the effects caused by more intense combustion

3.2. Analyses of archaeological bones

The initial evaluation of burning temperatures achieved through visual inspection [12] of archaeological bone samples is reported in Table 5. Temperature evaluation for each sample was determined according to the color variations observed across their entire surface using the commonly procedure that they employ which consists of referring to color charts reported in [12], as explained

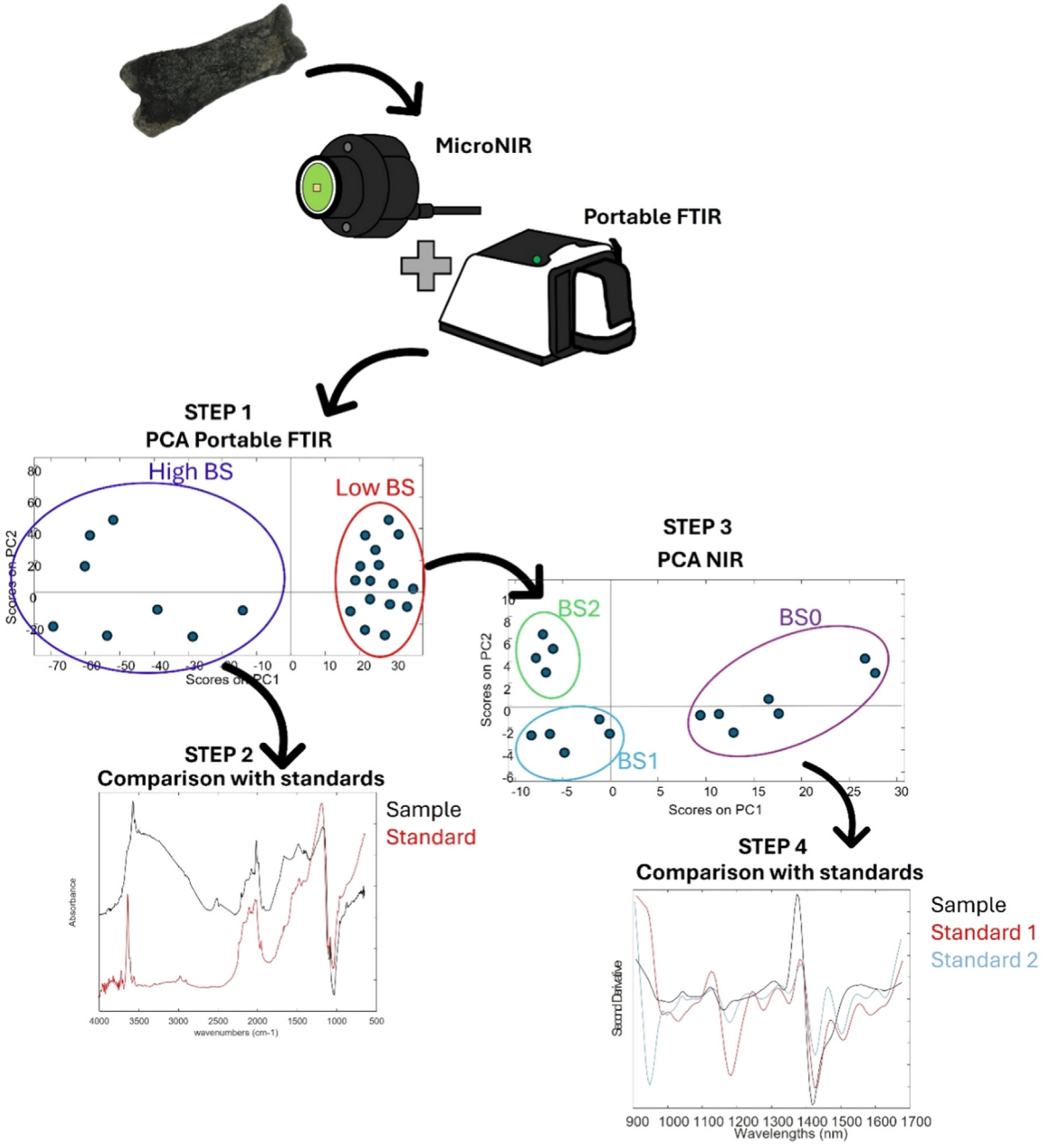

Fig. 1. The scheme of the approach followed during the analysis of archaeological samples.

in 2.2. In cases of sample heterogeneity, a broader temperature range was attributed, resulting in temperature assessments spanning from narrower ranges (e.g. M14) for more homogeneous samples, to wider ranges, sometimes encompassing a 600-degree span (e.g. M2). However, as reported in the previous paragraph (3.1) the state of burning depends not only on the temperature, but also on the duration of the exposure. Moreover, the bone color can be influenced by the burial environment and color perception by the operator. Since such assessment is mainly aimed at distinguishing the specimens based on their preservation state, subsequent spectroscopic investigation was conducted to find a more objective way to differentiate the samples. Spectra obtained with portable FTIR for some samples were particularly noisy, especially in the regions 1500–1700 cm^{-1} and 3200–3600 cm^{-1}, due to the influence of absorbed water. This is a significant limitation because these regions are important for distinguishing the best-preserved samples from those subjected to the strongest conditions and those in an intermediate state.

On the other hand, as observed in the standard samples, NIR may fail in the characterisation of samples in an intermediate state of conservation when the superficial darkening increases the absorption processes reducing the reflectance. For this reason, both portable FTIR and micro NIR analyses have been performed, and their results were interpreted in an integrated way with the approach that for the sake of clarity is summarised in the following steps (Fig. 1):

1. PCA analyses performed on FTIR data to distinguish samples in a worst conservation state (BS>5).
2. Identification of samples in worst conservation stats (BS5-BS6) based on the comparison of their spectral features with standard samples.

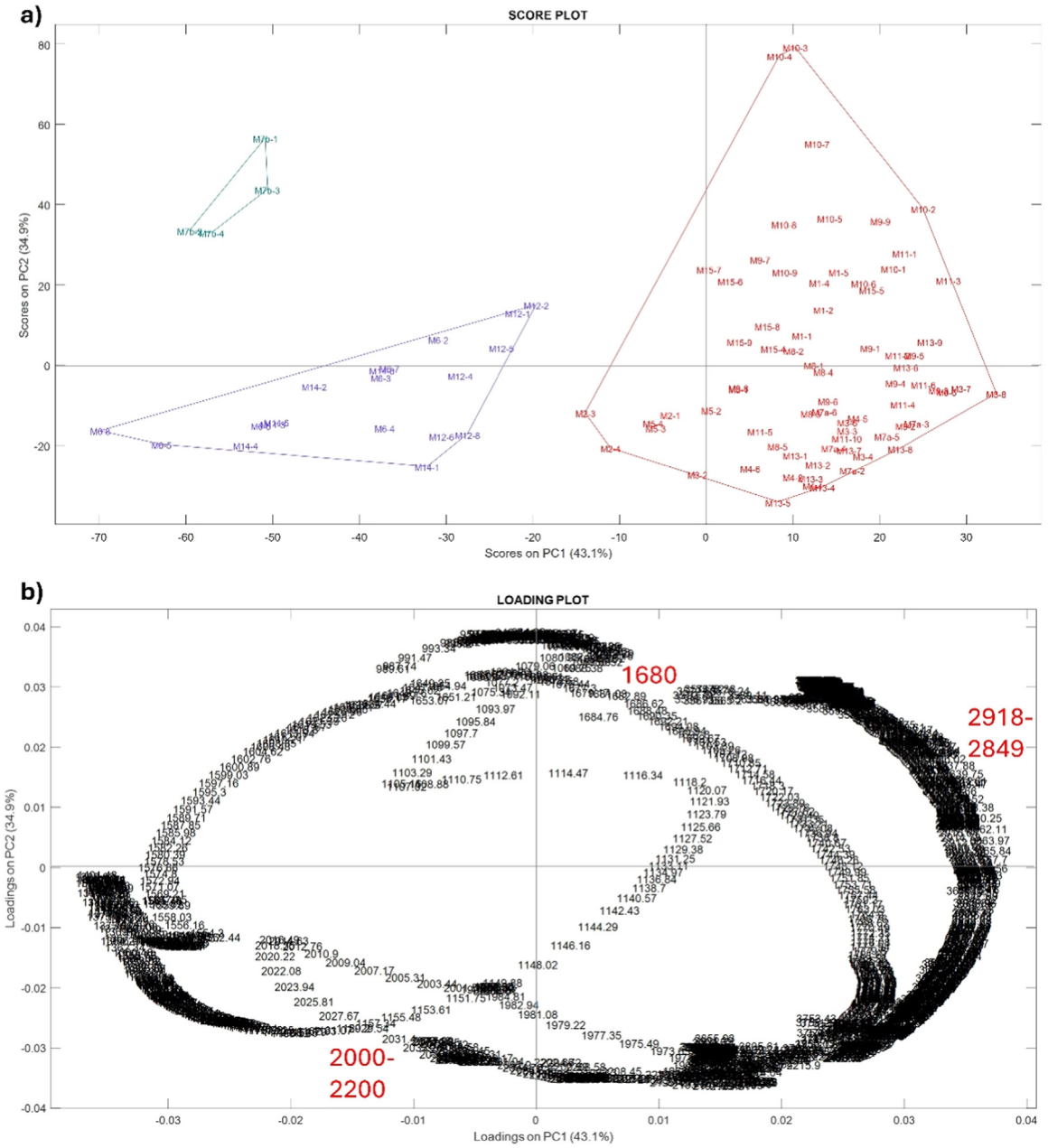

Fig. 2. PCA on mid IR data. The score plot (a) shows the separation of the samples in 3 groups according to the PC1 and PC2 wavenumbers, reported in the loading plot (b). The red group is constituted by samples with burning stage lower than BS5, the blue samples were identified as BS5–6 and the green ones as B6 according to the spectra.

3. PCA performed on NIR spectra acquired on the samples in the best conservation states (BS<5).
4. Identification of specimens in BS0-BS2 based on the comparison of their spectral features with standard samples.

3.2.1. Identification of samples in the worst conservation state: STEP 1–2 (PCA on FTIR data and integrated interpretation of FTIR and NIR data)

Portable FTIR data were submitted to PCA, revealing the discrimination among samples M7b, M6, M12 and M14 in the PC1-PC2 score plot (Fig. 2a). These samples are characterized by negative value on PC1, while all the other samples are distributed at positive values of PC1. The loading plot (Fig. 2b) highlights the variables that influence the distribution of samples along the different principal components (PCs).

According to the loadings scatter plot, negative PC1 values are associated with bands in the 2000–2200 cm^{-1} range, attributed to cyanate and cyanamide groups, which are characteristic of specimens in a more advanced state of degradation. In contrast, positive PC1 values correspond to CH stretching bands at 2918 and 2849 cm^{-1}, suggesting that the corresponding group of samples is in a more preserved state.

Sample M7b can be distinctly discriminated from all the others, as confirmed by the presence in the spectra of bands at 3571, 3544, and 3496 cm^{-1}, respectively related to OH vibration, ν(F-OH), and Cl–OH vibration (Fig. 3a), indicating a low conservation state characteristic of samples exposed to high level of thermal degradation (BS6) (Fig. 3b). The shape of the phosphate peak which became doubled and is shifted to higher wavenumbers (1044 cm^{-1}) indicates that, at this burning stage, bioapatite is dehydroxylated, has lost its thermal stability, and β-TCP is produced. The persistence of

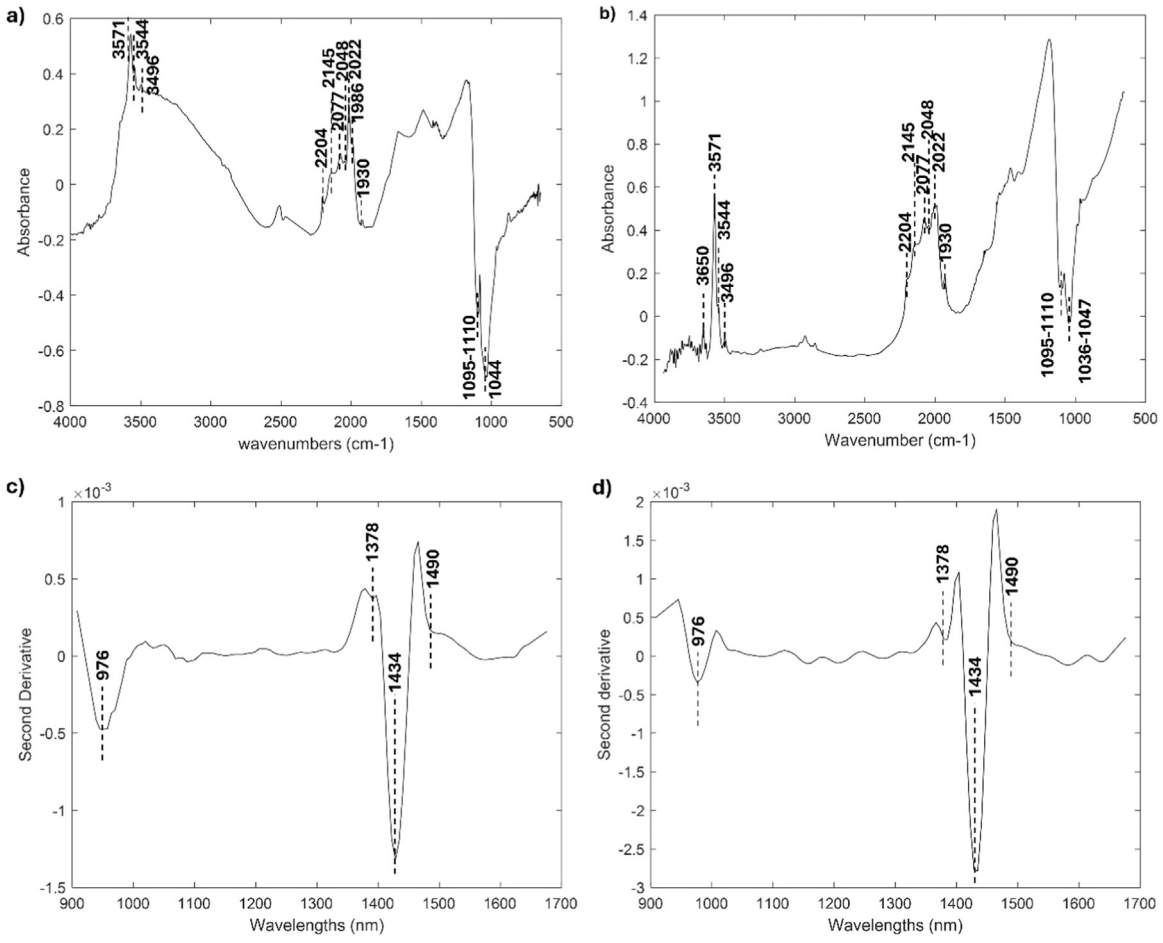

Fig. 3. Pre-processed average spectrum of spectra acquired on sample M7b by portable FTIR (a) and MicroNIR (c). Comparison with standard S17 acquire by portable FTIR (b) and MicroNIR (d).

cyanamide (2022 cm^{-1}, NCN^{2-}) and cyanate (NCO^{-}) band at 2204 cm^{-1} suggests that the sample has been burnt at high temperatures for long durations (BS6, standard treated at 900 °C for >60 min and over).

The same attribution can be obtained considering the NIR spectrum (Fig. 3c) which presents the same features observed in the standard S17 (BS6) such as the absence of the peak at 1007 nm, related to combination of δ H–O-H + ν O–H, the appearance of a shoulder at 1490 nm, which is ascribable to the Mg-OH 1st overtone, and of a small band at 1378 nm, due to the carbonation process and the re-crystallization of bioapatite. In addition, the 1434 nm band appears sharp, suggesting a higher level of burning and thus the increasing of crystallinity.

In samples M6 (Fig. S21), M12, and M14, FTIR bands attributed to NCO^{-} and NCN^{2-} at 2202 and 2022 cm^{-1} were detected, together with a weak band at 3578 cm^{-1}, related to OH vibration, as what was observed on standard S10 (BS5). However, the split of the phosphate peak related to $\nu_3(PO_4)^{3-}$ is clearly observed (1034, 1110 cm^{-1}) which can be attributed to a higher burning state (S17, BS6). For this reason, based on the portable FTIR results, the sample may be ascribed to an intermediate state between BS5 and BS6. In this case the NIR spectra appear quite noisy suggesting that the calcination is still not completely reached at least in depth (data not reported).

3.2.2. Identification of the best conservation states samples: STEP 3–4 (PCA on NIR data and interpretation of the spectra)

Samples located at positive values of PC1 in the score plot of portable FTIR data, reported in Fig. 2a, are correlated with the CH stretching at 2918 and 2849 cm^{-1} suggesting that they are in a better conservation state with the presence of organic substance. However, FTIR spectra of samples M1, M2, M3, M4, M5, M7a, M8, M9, M11, M13, M15, appear particularly noisy in the amide I and II region, and the absence of other specific markers of burning do not allow for a clear distinction among the different conservation states (Fig. S23, S24, S25, S26, S27, S28, S29, S30).

Sample M10 can be separated in the score plot (Fig. 2a) from the other samples due to the contribution of the band at 1680 cm^{-1} (Fig. 2b). Indeed, its FTIR averaged spectrum (Fig. S22) characterised by the presence of a strong and broad signal at 1688 cm^{-1} (amide I, or more likely, to aromatic $C = C$ and/or water bending modes), of the CH stretching vibrations (2918 and 2851 cm^{-1}), such as by the absence of cyanamide but the slight presence of cyanate (2210 cm^{-1}), suggest that this sample could be close to S3–5 (BS1–2).

To better distinguish the high conservation states samples, PCA has been performed on their NIR spectra.

Indeed, as already observed in standard samples, NIR spectroscopy, thanks to its higher penetration depth, offered better differentiation for samples exposed to milder conditions where the presence of organic materials is still detected.

The PC1–PC2 score plot revealed a separation of samples M3, M4, and M8 along the positive axis of PC1 (Fig. 4). The loadings on PC1–PC2 show a positive correlation with the bands at 1267 nm and 1025 nm, related to CH and NH 2nd overtones, respectively. This suggests that, moving from negative to positive PC1 values, the preservation of organic substances tends to increase.

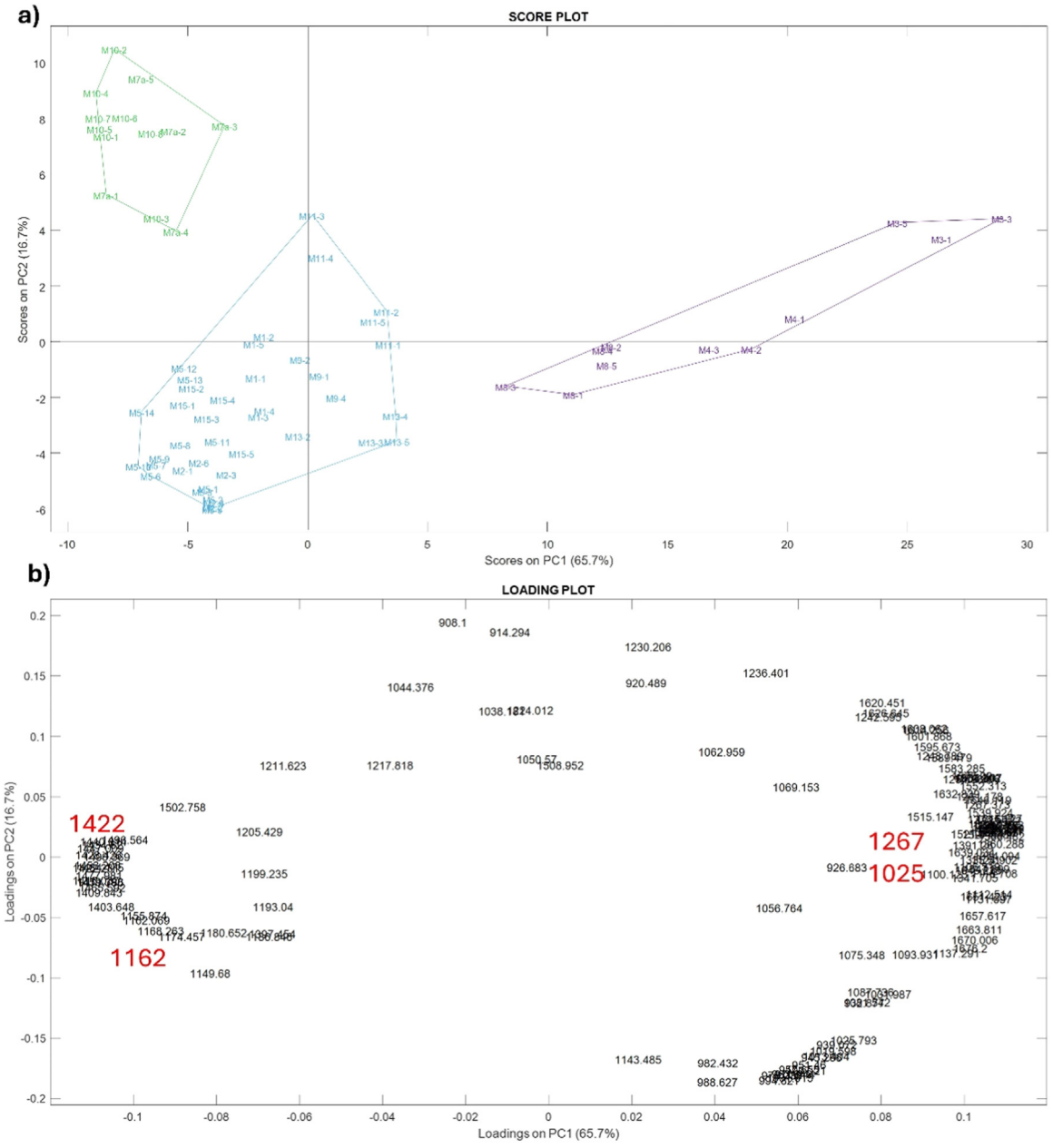

Fig. 4. PCA on MicroNIR data. a) PC1-PC2 score plot, b) PC1-PC2 loadings plot. The purple group is constituted by samples identified as burning stage B0–1 according to the spectra, the light blue ones as BS1 and the green ones as BS2.

In the spectra of samples M3, M4, and M8 (Fig. 5) even if the bands at 1583 (NH 1st overtone) and 1508 nm (NH 2nd overtone) cannot be clearly distinguished from the broad signal of the OH at 1422 nm, the presence of organic substance is confirmed by the CH 2nd overtone, which appears shifted at 1162 nm with respect to the standards as reported in [54], probably due to effects connected to the burial conditions. The peak at 1273 nm was not distinctly detected, instead, a slight broad signal was revealed at 1267 nm. If compared to the standards at low burning state S2 and S3 the signal of the organic components appears reduced in intensity, but this may be related to the fact that the real bones, besides the exposure to the burning conditions, were buried for a long time differently from the standards, and this may have affected their integrity. In M3 and M4, the band at 951 nm (ascribable to C–H 3rd overtone and/or O–H 2nd overtone) is not present, as in S2 (BS0), while a broad signal at 1007 nm (ascribable to combination of δ H–O-*H* + ν O–H) appears as in S3 (BS1) (Fig. 5). In M8 both signals can be clearly distinguished, as in S3 (BS1). Moreover, the band at 1341 nm related to the CH combination (CH_3 – CH_2 – CH), can be detected in all the three samples. Thus, these three samples appear in an intermediate situation between S2 (BS0) and S3 (BS1), with M8 moving towards the first identified state of burning based on the standards analyzed at known burning conditions.

Samples M1, M2, M5, M9, M11, M13, and M15 (Fig. S33, S35, S37, S38, S39, S40) present spectra with features common to S3 (BS1) (Fig. S31). The signals at 1422 nm (OH 1st overtone) is still present, as the peak at 1162 nm (CH 2nd overtone) in some samples (M9, M13, M15), even if the shape appears changed and the intensity is drastically reduced. It is noteworthy that the shape of the bands can be related to the morphology of the surface, which may have been altered not only by the combustion process but

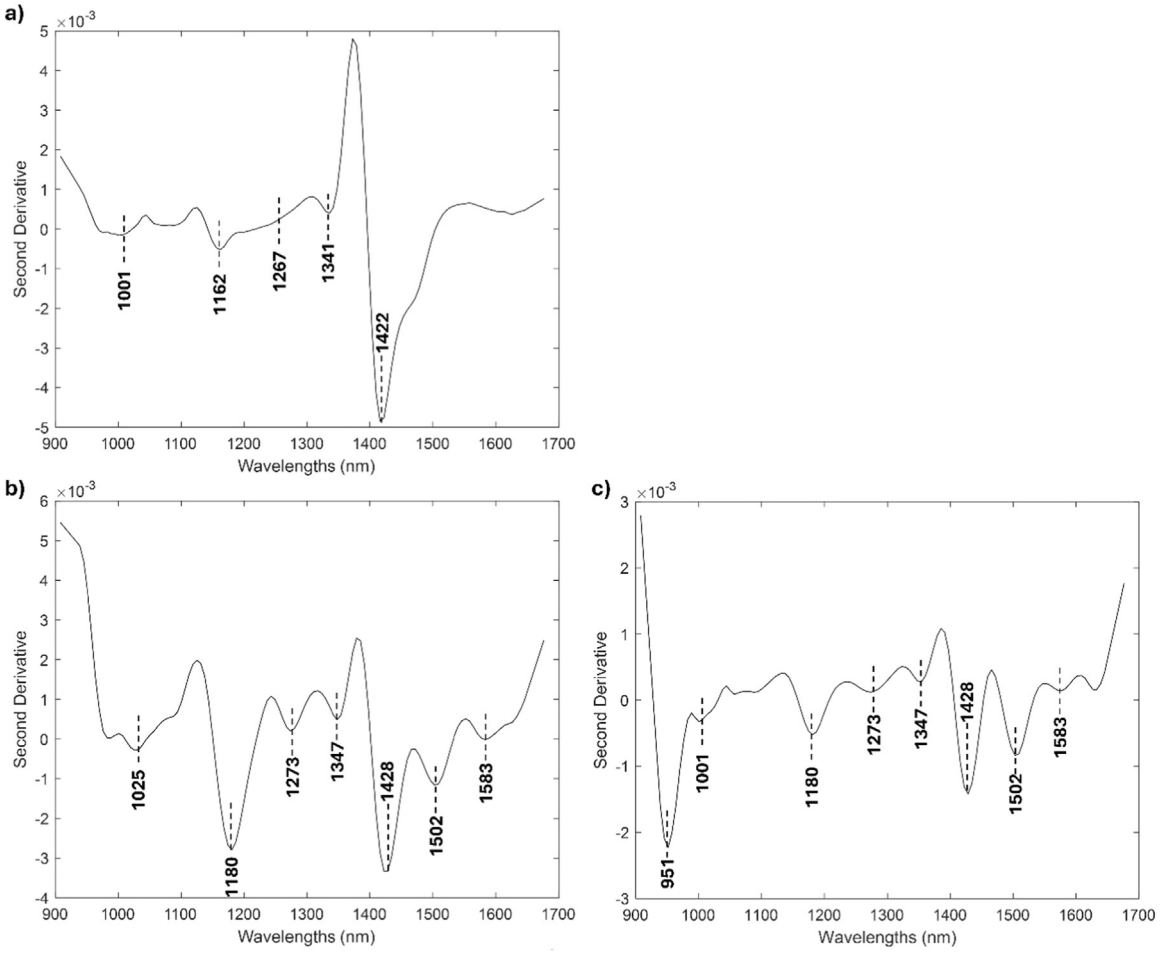

Fig. 5. Pre-processed averaged MicroNIR spectrum of spectra acquired on M3 (a), reported here as example for the first group of samples identified in the PCA. The spectra of M4 and M8 are reported in Fig. S34 b, S37 a. Comparison with the references S2 (BS0) (b) and S3 (BS1) (c) MicroNIR spectra.

also by the burial conditions. Moreover, sharper peaks are detected at 951 (C–H 3rd overtone and/or O–H 2nd overtone) and 1007 nm (combination of δ H–O-H + ν O–H).

Samples M7a and M10 (Fig. S36, S38) can be distinguished along PC2. Compared to the previous samples, the intensity of the signals in the range 1400–1600 nm is strongly reduced, and only the peaks at 1007 and 951 nm can be clearly detected in addition to the OH stretching at 1422 nm, similar to standard S4 and S5 (BS2) (Fig. S32).

3.2.3. Discussions of the results

By comparing the results reported in Table 5, it can be noted that confiding just on the visual assessment provides ambiguous results if the aim of defining the burning state is to perform a pre-screening of the more preserved samples for other destructive analyses. Indeed, it is known that organic matter is degraded and lost when bones are exposed to a wide range of temperatures (300–800 °C) depending, as demonstrated in this study and in previous research [2], not only by temperature but also by the duration of the exposure.

The integration of the two spectroscopic approaches can improve the determination of the burning stages of bones. Specifically, mid-IR proved valuable in identifying stages in samples burnt above 600 °C due to the gradual disappearance of the organic fraction and the emergence of specific markers o However, in the early stages, due to the high noise in the amide region, it may be difficult to establish specific changes and a clear distinction of samples in burning state from BS0 to BS2 was not possible. As reported in paragraph 3.1. standards in the BS2 states present a high reduction of the organic content thus it may be quite useful to discriminate them with respect to samples which can be identified as belonging to BS0-BS1. Near-IR, within the 900–1700 nm range, more effectively detects variations in the early combustion stage. Therefore, by combining these methods, it is possible to identify bones that are better preserved for subsequent destructive analyses.

From an archaeological perspective, the integration of portable FTIR and MicroNIR spectrometers, combined with chemometric approaches, offers a more rigorous and scientifically grounded assessment of the degree of thermal alteration in archaeological materials. This integrated methodology enhances our ability to clearly distinguish between different stages of burning, contributing to a more nuanced understanding of pyro technological processes.

Such precise characterization is particularly valuable in funerary contexts, as it enables a careful evaluation of each sample prior to any decision to discard it on the basis of being “too burnt.” In doing so, it minimizes the risk of excluding materials that, despite their altered appearance, may still retain valuable information about ancient funerary practices.

In this specific case, the integration of these two non-destructive techniques proved especially effective, allowing the identification of samples M3 and M4 as the best preserved. These samples were determined to be the most suitable candidates for further analysis using micro-destructive techniques, thus ensuring that research efforts are focused on material with the highest potential for meaningful results [55].

4. Conclusions

This study represents a significant step forward in the analytical investigation of burnt human remains. Traditionally, archaeologists have relied on visual assessment and color evaluation to estimate the degree of thermal alteration in bones. However, as demonstrated here, such methods can often lead to ambiguous or misleading conclusions, as color changes are influenced not only by temperature but also by burning duration and environmental conditions.

To overcome these limitations, this study proposes the integration of portable FTIR and MicroNIR spectrometers combined with chemometric techniques, offering a more scientific and objective approach to evaluate thermal alteration. This integrated methodology allows to assess each individual sample before it is potentially discarded for being "too burnt," thereby minimizing the risk of overlooking material that could yield significant insights into funerary practices.

Portable FTIR spectroscopy has proven highly effective in characterizing the molecular composition of thermally altered bones, particularly in identifying advanced burning stages where characteristic mineralogical transformations occur. However, its ability to detect early-stage burning is limited by the interference of water, which can overcome modifications related to the proteinaceous components.

MicroNIR, on the other hand, has been effective in identifying bones affected by early burning -stage. Thanks to its deeper penetration, this technique is less influenced by surface contamination and better suited to detect organic subsurface preservation. Nevertheless, its effectiveness decreases as charring increases, due to the significant reduction in signal intensity.

The application of Principal Component Analysis (PCA) to both FTIR and NIR datasets proved effective in extracting complementary information from the two techniques. PCA on FTIR data successfully distinguished samples in advanced burning stages, though it failed to clearly separate early-stage samples. Conversely, PCA on NIR spectra allowed for the identification of better-preserved samples in earlier stages of burning.

By combining FTIR (mid-IR) and NIR spectroscopy with multivariate statistical analysis, this study proposes a reliable protocol for in-situ prescreening of burnt bone samples.

These innovative methods open new avenues for the study of burnt remains, which have traditionally been analyzed only through classical physical anthropology approaches. As a result, important information may have been lost—information crucial to understanding burial practices, reconstructing the paleodemographic profile of past populations, and exploring the cultural and social dynamics of ancient communities.

This work represents a first feasibility study. Future research on a broader range of modern experimental samples, subjected to different burning conditions, could lead to the development of supervised classification models based on temperature and exposure time. Additionally, the application of hyperspectral imaging systems may further enhance the detection of heterogeneous chemical changes in burnt bones, providing more accurate information for the identification of the sampling area inside the specimen.

Funding

This work has been partially financially supported by the Slovenian Research and Innovation Agency (ARIS); research project (grant) J7-50226 and by the project PE5 CHANGES: Cultural Heritage Active Innovation for Sustainable Society. PE 0000020 CHANGES, - CUP B53C22003780006, PNRR Missione 4 Componente 2 Investimento 1.3, NextGenerationEU

Acknowledgments

We thank the Soprintendenza Archeologia, Belle Arti e Paesaggio per la Città Metropolitana di Bologna e le province di Modena, Reggio Emilia e Ferrara, and Cinzia Cavallari for initiating the research project on the Funeral Rituals of *Mutina*. We thank Museo Civico di Modena, particularly Silvia Pellegrini, for permission to study and access the materials. The authors would like to thank the Slovenian Research and Innovation Agency (ARIS) for supporting this work through grant J7-50226.

Supplementary materials

Supplementary material associated with this article can be found, in the online version, at doi:10.1016/j.culher.2025.07.021.

References

[1] C. Snoeck, J.A. Lee-Thorp, R.J. Schulting, From bone to ash: compositional and structural changes in burned modern and archaeological bone, Palaeogeogr. Palaeoclimatol. Palaeoecol. 416 (2014) 55–68, doi:10.1016/j.palaeo.2014.08.002.
[2] L. Legan, T. Leskovar, M. Črešnar, F. Cavalli, D. Innocenti, P. Ropret, Non-invasive reflection FTIR characterization of archaeological burnt bones: reference database and case studies, J. Cult. Herit. 41 (2020) 13–26, doi:10.1016/j.culher.2019.07.006.
[3] A.C. Power, J. Chapman, S. Chandra, J.J. Roberts, D. Cozzolino, Illuminating the flesh of bone identification – An application of near infrared spectroscopy, Vib. Spectrosc. 98 (2018) 64–68, doi:10.1016/j.vibspec.2018.07.011.
[4] E. Catelli, G. Sciutto, S. Prati, M.V. Chavez Lozano, L. Gatti, F. Lugli, S. Silvestrini, S. Benazzi, E. Genorini, R. Mazzeo, A new miniaturised short-wave infrared (SWIR) spectrometer for on-site cultural heritage investigations, Talanta 218 (2020) 121112, doi:10.1016/j.talanta.2020.121112.
[5] J.D. Fredericks, P. Bennett, A. Williams, K.D. Rogers, FTIR spectroscopy: a new diagnostic tool to aid DNA analysis from heated bone, Forensic Sci. Int. Genet. 6 (2012) 375–380, doi:10.1016/j.fsigen.2011.07.014.
[6] S.H. Bayarı, K. Özdemir, E.H. Sen, C. Araujo-Andrade, Y.S. Erdal, Application of ATR-FTIR spectroscopy and chemometrics for the discrimination of human bone remains from different archaeological sites in Turkey, Spectrochim. Acta - Part A Mol. Biomol. Spectrosc. 237 (2020), doi:10.1016/j.saa.2020.118311.
[7] G. Dal Sasso, M. Lebon, I. Angelini, L. Maritan, D. Usai, G. Artioli, Bone diagenesis variability among multiple burial phases at Al Khiday (Sudan) investigated by ATR-FTIR spectroscopy, Palaeogeogr. Palaeoclimatol. Palaeoecol. 463 (2016) 168–179, doi:10.1016/j.palaeo.2016.10.005.
[8] M.M. Figueiredo, J.A.F. Gamelas, A.G. Martins, Characterization of bone and bone-based graft materials using FTIR spectroscopy, Infrared Spectrosc. - Life Biomed. Sci. (2012), doi:10.5772/36379.
[9] C. Kendall, A.M.H. Eriksen, I. Kontopoulos, M.J. Collins, G. Turner-Walker, A. Marie, H. Eriksen, M.J. Collins, G. Turner-Walker, I. Kontopoulos, A.M.H. Eriksen, I. Kontopoulos, M.J. Collins, G. Turner-Walker, Diagenesis of archaeological bone and tooth, Palaeogeogr. Palaeoclimatol. Palaeoecol. 491 (2018) 21–37, doi:10.1016/j.palaeo.2017.11.041.
[10] E. Stamataki, I. Kontopoulos, K. Salesse, R. McMillan, B. Veselka, C. Sabaux, R. Annaert, M. Boudin, G. Capuzzo, P. Claeys, S. Dalle, M. Hlad, A. Sengeløv, M. Vercauteren, E. Warmenbol, D. Tys, G. De Mulder, C. Snoeck, Is it hot enough? A multi-proxy approach shows variations in cremation conditions during the Metal Ages in Belgium, J. Archaeol. Sci. 136 (2021), doi:10.1016/j.jas.2021.105509.
[11] J. Rosa, A.R. Vassalo, A. Amarante, L.A.E. Batista de Carvalho, M.P.M. Marques, M.T. Ferreira, D. Gonçalves, Burned and buried: a vibrational spectroscopy analysis of burial-related diagenetic changes of heat-altered human bones, Am. J. Biol. Anthropol. 180 (2023) 534–547, doi:10.1002/ajpa.24691.
[12] P.L. Walker, K.W.P. Miller, R. Richman, Time, temperature, and oxygen availability: an experimental study of the effects of environmental conditions on the color and organic content of cremated bone, Anal. Burn. Hum. Remain. (2008) 129–135.
[13] F. Berna, A. Matthews, S. Weiner, Solubilities of bone mineral from archaeological sites: the recrystallization window, J. Archaeol. Sci. 31 (2004) 867–882, doi:10.1016/j.jas.2003.12.003.
[14] M.M. Cascant, S. Rubio, G. Gallello, A. Pastor, S. Garrigues, M. de la Guardia, Burned bones forensic investigations employing near infrared spectroscopy, Vib. Spectrosc. 90 (2017) 21–30, doi:10.1016/j.vibspec.2017.02.005.
[15] G. Capuzzo, C. Snoeck, M. Boudin, S. Dalle, R. Annaert, M. Hlad, I. Kontopoulos, C. Sabaux, K. Salesse, A. Sengelov, E. Stamataki, B. Veselka, E. Warmenbol, G. De Mulder, D. Tys, M. Vercauteren, Cremation vs. inhumation: modeling cultural changes in funerary practices from the mesolithic to the middle ages in belgium using kernel density analysis on 14C data, Radiocarbon 62 (2020) 1809–1832, doi:10.1017/RDC.2020.88.
[16] G. Capuzzo, G. De Mulder, C. Sabaux, S. Dalle, M. Boudin, R. Annaert, M. Hlad, K. Salesse, A. Sengelov, E. Stamataki, B. Veselka, E. Warmenbol, C. Snoeck, M. Vercauteren, Final neolithic and bronze age funerary practices and population dynamics in Belgium, the impact of radiocarbon dating cremated bones, Radiocarbon 65 (2023) 51–80, doi:10.1017/RDC.2022.94.

[17] T.J.U. Thompson, M. Islam, K. Piduru, A. Marcel, An investigation into the internal and external variables acting on crystallinity index using Fourier Transform Infrared spectroscopy on unaltered and burned bone, Palaeogeogr. Palaeoclimatol. Palaeoecol. 299 (2011) 168–174, doi:10.1016/j.palaeo.2010.10.044.
[18] L.D. Mkukuma, J.M.S. Skakle, I.R. Gibson, C.T. Imrie, R.M. Aspden, D.W.L. Hukins, Effect of the proportion of organic material in bone on thermal decomposition of bone mineral: an investigation of a variety of bones from different species using thermogravimetric analysis coupled to mass spectrometry, high-temperature X-ray diffraction, Calcif. Tissue Int. 75 (2004) 321–328, doi:10.1007/s00223-004-0199-5.
[19] P. Shipman, G. Foster, M. Schoeninger, Burnt bones and teeth: an experimental study of color, morphology, crystal structure and shrinkage, J. Archaeol. Sci. 11 (1984) 307–325, doi:10.1016/0305-4403(84)90013-X.
[20] E. Hosseinzadeh, M. Davarpanah, N.H. Nemati, S.A. Tavakoli, Fabrication of a hard tissue replacement using natural hydroxyapatite derived from bovine bones by thermal decomposition method, Int. J. Organ Transplant. Med. 5 (2014) 23–31.
[21] M. Van Strydonck, M. Boudin, M. Hoefkens, G. De Mulder, 14C-dating of cremated bones, why does it work?, LUNULA (Bruxelles) (2005) 3–10.
[22] J. Olsen, J. Heinemeier, P. Bennike, C. Krause, K.Margrethe Hornstrup, H. Thrane, Characterisation and blind testing of radiocarbon dating of cremated bone, J. Archaeol. Sci. 35 (2008) 791–800, doi:10.1016/j.jas.2007.06.011.
[23] C. Sabaux, C. Snoeck, G. Capuzzo, B. Veselka, S. Dalle, E. Warmenbol, E. Stamataki, M. Hlad, A. Sengeløv, V. Debaille, M. Boudin, K. Salesse, R. Annaert, M. Vercauteren, G. De Mulder, Novel multidisciplinary approach detects multiple individuals within the same Late Bronze-early Iron Age cremation graves, Radiocarbon (2024) 761–773, doi:10.1017/RDC.2024.82.
[24] M. Greiner, A. Rodríguez-Navarro, M.F. Heinig, K. Mayer, B. Kocsis, A. Göhring, A. Toncala, G. Grupe, W.W. Schmahl, Bone incineration: an experimental study on mineral structure, colour and crystalline state, J. Archaeol. Sci. Reports. 25 (2019) 507–518, doi:10.1016/j.jasrep.2019.05.009.
[25] J.B. Devlin, N.P. Herrmann, Bone color as an interpretive tool of the depositional history of archaeological cremains, Anal. Burn. Hum. Remain. (2008), doi:10.1016/B978-012372510-3.50008-3.
[26] T. Krap, J.M. Ruijter, K. Nota, J. Karel, A.L. Burgers, M.C.G. Aalders, R.J. Oostra, W. Duijst, Colourimetric analysis of thermally altered human bone samples, Sci. Rep. 9 (2019) 1–10, doi:10.1038/s41598-019-45420-8.
[27] L. Rubio, R. Díaz-Vico, I. Smith-Fernández, A. Smith-Fernández, J. Suárez, S. Martin-De-las-heras, I. Santos, Spectrophotometric color measurement to assess temperature of exposure in cortical and medullar heated human bones: a preliminary study, Diagnostics 10 (2020), doi:10.3390/diagnostics10110979.
[28] S.K.T.S. Wärmländer, L. Varul, J. Koskinen, R. Saage, S. Schlager, Estimating the temperature of heat-exposed bone via machine learning analysis of SCI color values: a pilot study, J. Forensic Sci. 64 (2019) 190–195, doi:10.1111/1556-4029.13858.
[29] K.E. Squires, T.J.U. Thompson, M. Islam, A. Chamberlain, The application of histomorphometry and Fourier transform infrared spectroscopy to the analysis of early Anglo-Saxon burned bone, J. Archaeol. Sci. 38 (2011) 2399–2409, doi:10.1016/j.jas.2011.04.025.
[30] F. Seghi, F. Lugli, H.F. James, T. Löffelmann, E. Armaroli, A. Vazzana, A. Cipriani, C. Snoeck, S. Benazzi, Strontium isotopes and cremation: investigating mobility patterns in the Roman city of Mutina (north-eastern Italy), J. Archaeol. Sci. Reports. 58 (2024), doi:10.1016/j.jasrep.2024.104728.
[31] C. Snoeck, C. Cheung, J.I. Griffith, H.F. James, K. Salesse, Strontium isotope analyses of archaeological cremated remains – new data and perspectives, Data Br 42 (2022) 108115, doi:10.1016/j.dib.2022.108115.
[32] L. Waltenberger, M.D. Bosch, M. Fritzl, A. Gahleitner, C. Kurzmann, M. Piniel, R.B. Salisbury, L. Strnad, H. Skerjanz, D. Verdianu, C. Snoeck, F. Kanz, K. Rebay-Salisbury, More than urns: a multi-method pipeline for analyzing cremation burials, PLoS One 18 (2023) 1–27, doi:10.1371/journal.pone.0289140.
[33] G.Pothier Bouchard, S.M. Mentzer, J. Riel-Salvatore, J. Hodgkins, C.E. Miller, F. Negrino, R. Wogelius, M. Buckley, Portable FTIR for on-site screening of archaeological bone intended for ZooMS collagen fingerprint analysis, J. Archaeol. Sci. Reports. 26 (2019) 101862, doi:10.1016/j.jasrep.2019.05.027.
[34] S. Weiner, P. Goldberg, O. Bar-Yosef, Bone preservation in Kebara Cave Israel, J. Archaeol. Sci. 20 (1993) 613–627.
[35] D.H. Butler, P.C. Dawson, Accessing Hunter-Gatherer site structures using fourier transform infrared spectroscopy: applications at a Taltheilei settlement in the Canadian Sub-Arctic, J. Archaeol. Sci. 40 (2013) 1731–1742, doi:10.1016/j.jas.2012.11.015.
[36] I. Kontopoulos, K. Penkman, V.E. Mullin, L. Winkelbach, M. Unterländer, A. Scheu, S. Kreutzer, H.B. Hansen, A. Margaryan, M.D. Teasdale, B. Gehlen, M. Street, N. Lynnerup, I. Liritzis, A. Sampson, C. Papageorgopoulou, M.E. Allentoft, J. Burger, D.G. Bradley, M.J. Collins, Screening archaeological bone for palaeogenetic and palaeoproteomic studies, PLoS One 15 (2020) 1–17, doi:10.1371/journal.pone.0235146.
[37] M. Pal Chowdhury, K.D. Choudhury, G.P. Bouchard, J. Riel-Salvatore, F. Negrino, S. Benazzi, L. Slimak, B. Frasier, V. Szabo, R. Harrison, G. Hambrecht, A.C. Kitchener, R.A. Wogelius, M. Buckley, Machine learning ATR-FTIR spectroscopy data for the screening of collagen for ZooMS analysis and mtDNA in archaeological bone, J. Archaeol. Sci. 126 (2021), doi:10.1016/j.jas.2020.105311.
[38] M.P.M. Marques, D. Gonçalves, A.P. Mamede, T. Coutinho, E. Cunha, W. Kockelmann, S.F. Parker, L.A.E. Batista de Carvalho, Profiling of human burned bones: oxidising versus reducing conditions, Sci. Rep. 11 (2021) 1–13, doi:10.1038/s41598-020-80462-3.
[39] K. Salesse, E. Stamataki, I. Kontopoulos, G. Verly, R. Annaert, M. Boudin, G. Capuzzo, P. Claeys, S. Dalle, M. Hlad, G. de Mulder, C. Sabaux, A. Sengeløv, B. Veselka, E. Warmenbol, M. Vercauteren, C. Snoeck, These boots are made for burnin': inferring the position of the corpse and the presence of leather footwears during cremation through isotope (δ13C, δ18O) and infrared (FTIR) analyses of experimentally burnt skeletal remains, PLoS One 16 (2021) 1–22, doi:10.1371/journal.pone.0257199.
[40] T.J.U. Thompson, M. Gauthier, M. Islam, The application of a new method of Fourier Transform Infrared spectroscopy to the analysis of burned bone, J. Archaeol. Sci. 36 (2009) 910–914, doi:10.1016/j.jas.2008.11.013.
[41] F.H. Reidsma, A. Van Hoesel, B.J.H. Van Os, L. Megens, F. Braadbaart, Charred bone : physical and chemical changes during laboratory simulated heating under reducing conditions and its relevance for the study of fire use in archaeology Journal of Archaeological Science : reports Charred bone : physical and chemical changes, J. Archeolog. Sci.: Rep. 10 (2018) 282–292, doi:10.1016/j.jasrep.2016.10.001.
[42] R.A. Crocombe, P.E. Leary, B.W. Kammrath, Portable Spectroscopy and Spectrometry, John Wiley and Sons Ltd, 2021. https://doi.org/10.1002/9781119636489.
[43] E.H. Korte, A. Röseler, Infrared reststrahlen revisited: commonly disregarded optical details related to n<1, Anal. Bioanal. Chem. 382 (2005) 1987–1992, doi:10.1007/s00216-005-3407-x.
[44] D. Vincke, R. Miller, É. Stassart, M. Otte, P. Dardenne, M. Collins, K. Wilkinson, J. Stewart, V. Baeten, J. Antonio, F. Pierna, J.A. Fernández Pierna, Analysis of collagen preservation in bones recovered in archaeological contexts using NIR Hyperspectral Imaging, Talanta 125 (2014) 181–188, doi:10.1016/j.talanta.2014.02.044.
[45] A.P. Mamede, D. Gonçalves, M.P.M. Marques, L.A.E. Batista de Carvalho, Burned bones tell their own stories: a review of methodological approaches to assess heat-induced diagenesis, Appl. Spectrosc. Rev. 53 (2018) 603–635, doi:10.1080/05704928.2017.1400442.
[46] A.P. Mamede, A.R. Vassalo, G. Piga, E. Cunha, S.F. Parker, M.P.M. Marques, L.A.E. Batista De Carvalho, D. Gonçalves, Potential of bioapatite hydroxyls for research on archeological burned bone, Anal. Chem. 90 (2018) 11556–11563, doi:10.1021/acs.analchem.8b02868.
[47] F. Lugli, G. Sciutto, P. Oliveri, C. Malegori, S. Prati, L. Gatti, S. Silvestrini, M. Romandini, E. Catelli, M. Casale, S. Talamo, P. Iacumin, S. Benazzi, R. Mazzeo, Near-infrared hyperspectral imaging (NIR-HSI) and normalized difference image (NDI) data processing: an advanced method to map collagen in archaeological bones, Talanta 226 (2021), doi:10.1016/j.talanta.2021.122126.
[48] C. Malegori, G. Sciutto, P. Oliveri, S. Prati, L. Gatti, E. Catelli, S. Benazzi, S. Cercatillo, D. Paleček, R. Mazzeo, S. Talamo, Near-infrared hyperspectral imaging to map collagen content in prehistoric bones for radiocarbon dating, Commun. Chem. 6 (2023) 1–10, doi:10.1038/s42004-023-00848-y.
[49] M. Sponheimer, C.M. Ryder, H. Fewlass, E.K. Smith, W.J. Pestle, Saving old bones : a non-destructive method for bone collagen prescreening, Sci. Rep. 9 (2019), doi:10.1038/s41598-019-50443-2.
[50] A.C. Power, J. Chapman, D. Cozzolino, Near infrared spectroscopy, the skeleton key for bone identification, Spectrosc. Eur. 30 (2018) 19–21.
[51] Y. Ozaki, C. Huck, S. Tsuchikawa, S.B. Engelsen, Near-infrared spectroscopy: theory, spectral analysis, instrumentation, and applications, Springer, Singapore, 2021.
[52] L. Yue, M. Monge, M.H. Ozgur, K. Murphy, S. Louie, C.A. Miller, A. Emami, M.S. Humayun, Simulation and measurement of transcranial near infrared light penetration, Opt. Interact. with Tissue Cells XXVI 9321 (2015) 93210S, doi:10.1117/12.2077019.
[53] M.V. Padalkar, N. Pleshkoa, Wavelength-dependent penetration depth of near infrared radiation into cartilage, Analyst (2015).
[54] S. Atanassova, D. Kostov, M. Stefanov, Near-infrared analysis and dating of archaeological bones, Pick. Up Good Vib (2013) 481.
[55] S. Christopher, S. Steven, The analysis of burned Human remains, Anal. Burn. Hum. Remain. (2008), doi:10.1016/B978-0-12-372510-3.X5001-1.